Article:

Gao, Yang, Xia, Hao, Sulaeman, Allyn P. et al. (3 more authors) (2019) Defibrillated celluloses via dual twin-screw extrusion and microwave hydrothermal treatment (MHT) of spent pea biomass. ACS Sustainable Chemistry & Engineering. ISSN 2168-0485

https://doi.org/10.1021/acssuschemeng.9b02440

ACS Sustainable Chemistry & Engineering

Article

Defibrillated celluloses via dual twin-screw extrusion and microwave hydrothermal treatment (MHT) of spent pea biomass

Yang Gao, Hao Xia, Allyn Sulaeman, Eduardo Macedo de Melo, Thomas Iain James Dugmore, and Avtar Singh Matharu

ACS Sustainable Chem. Eng., **Just Accepted Manuscript** • DOI: 10.1021/acssuschemeng.9b02440 • Publication Date (Web): 06 Jun 2019

Defibrillated celluloses via dual twin-screw extrusion and microwave hydrothermal treatment (MHT) of spent pea biomass

*Yang Gao†, Hao Xia†, Allyn P. Sulaeman†, Eduardo M. de Melo†, Tom I.J. Dugmore† and Avtar S. Matharu†**

†Green Chemistry Centre of Excellence, Department of Chemistry, University of York, York YO10 5DD. UK

Corresponding Author (s):

Avtar Matharu

Green Chemistry Centre of Excellence, Department of Chemistry, University of York, York YO10 5DD. UK.

* E-mail: avtar.matharu@york.ac.uk

ABSTRACT: The defibrillation of lignocellulosic matter from pea waste using a dual approach of twin-screw extrusion and microwave hydrothermal treatment (MHT) in the presence of water alone from 120 to 200 ^{o}C is reported. Gradual "scissoring" of biomass macrofibres to microfibrils was observed alluding to the Hy-MASS (*Hydrothermal Microwave-assisted Selective Scissoring*) concept. The morphology and properties of two types of MFC: PEA (non-extruded) and EPEA (extruded) were compared. The EPEA samples gave higher crystallinity index and thermal stability, reduced lignin and hemicellulose content, narrower fibril width, better water holding capacity slightly and higher surface area compared with their non-extruded counterparts (PEA). Twin screw extrusion as a pretreatment method followed by MHT represents a potential way to produce microfibrillated cellulose with improved physical performance from complex biomass sources.

KEYWORDS: microfibrillated cellulose, spent pea biomass (haulm), hydrothermal microwave treatment, twin-screw extrusion

INTRODUCTION

As the second most important legume after the common green bean,[1] peas (*Pisum sativum*) are grown widely all over the world.[2] In 2017, 40 thousand hectares of peas were grown in the UK, yielding an average of 4 tons per hectare.[3] In general, more than 30% (w/w) waste is produced during pea harvesting, which is often left on farmland.[4] Anecdotally, more than enough pea waste is left on land maintaining soil health and nutrition. Thus, there is an excess which serves no additional benefit and probably decays. Therefore, reutilization or valorization of unavoidable pea waste, e.g. leaves, vines, pods and stalks, (also known as haulm) represents a significant lignocellulosic resource for chemical and economic exploitation,[5] but also an opportunity to improve the environment by divert waste .[6-8, 13] Recently, nanocellulose has emerged as biomaterial with great promise because of its application in food,[9] electronics,[10] catalysis,[11] hydrocolloids,[12] biomedical materials[13,14] due to its excellent properties including high mechanical strength, high surface area and enhanced optical properties.[15,16] The high demand of nanocellulose is expected to expand the market size from USD 240.7 million in 2017 to USD 661.3 million by 2023 with a 18.4% growth rate.[17]

Nanocellulose is commonly described as nano-sized cellulose fibrils which are derived from plant cell walls or bacteria.[18] Generally, nanocellulose is classified into: i. nano-objects, namely, cellulose nanocrystals (CNC or NCC, width = 3-10 nm, aspect ratio = 5-50) and cellulose nanofibrils (CNF or NFC, width = 5-30 nm, aspect ratio>50); ii. nanostructured celluloses, namely, microcrystalline cellulose (CMC or MCC, width = 10-15 μm, aspect ratio<2), and; iii. microfibrillated cellulose (MFC or CMF, width = 10-100 nm, length=0.5-10 μm) according to TAPPI WI3021.[19,20]

Traditionally, nanocellulose is made from wood pulp. An extensive number of studies have been carried out on production of nanocellulose through conventional mineral acid-catalysed hydrolysis and/or enzymatic digestion followed by physical processing (e.g. ultrasound, mechanical shear).[21,22] However, such treatments are deemed energy- and time-consuming, costly and environmentally-hazardous but are necessary due to the inherent, stable, inter-twined structure of the lignocellulosic matrix.[23,24] Thus, pretreatment becomes one of the crucial techniques to change lignocellulosic biomass to high-value chemicals or materials.[25,26] During the (pre)treatment of lignocellulosic biomass, both the physical macro- and micro-structure and the chemical composition of the biomass changes.[27] For example, the degree of crystallinity of cellulose can be altered as amorphous lignin/hemicellulose which surrounds cellulose fibres are destroyed and the specific surface area (SSA) can be improved due to diminution of macrofibres.[28,29] Normally, the pretreatment process can be classified into chemical (*e.g.* acid, alkali, ionic liquid treatment),[30-34] physical (mechanical splintered, microwave, ultrasound),[35-37] biological (*e.g.* white rot fungi, brown rot fungi, enzymatic)[38] or physicochemical combined methods (*e.g.* steam explosion, CO_2 explosion).[39,40] Therefore, alternative methods for nanocellulose production have been sought, for example, Chen et al. [41] reported that the recyclable organic acid hydrolyzed lap pulp at atmospheric pressure to produce the CNC and CNF, Nurul et al.[42] produced CNC nanocellulose from catalytic ionic liquid hydrolysis, Prasad et al.[43] used fungus to prepare cellulose nanowhiskers (CNW) by hydrolysing the microcrystalline region of cellulose. Matharu et al. and de Melo et al. reported a novel acid-free microwave hydrothermal treatment (MHT) method to obtain pseudo-nanocellulosic fibrils and/or nanocrystals without any additional chemicals.[20,44]

Herein, the importance of this study is to explore the potential valorization of pea waste (rather than traditional wood pulp) as a source of defibrillated celluloses using twin screw extrusion as a pretreatment prior to microwave hydrothermal treatment (MHT) (Figure 1). Twin screw extrusion was selected as the pretreatment for being continuous, low cost, requiring no heat and the application of high shearing forces in the biomass[45] facilitates cell wall rupture and removal of non-cellulosic matter. The resultant physico-chemical properties of extruded pea waste (EPEA) will be compared with their non-extruded counterparts (PEA) so as to assess the influence of extrusion as a pretreatment method.

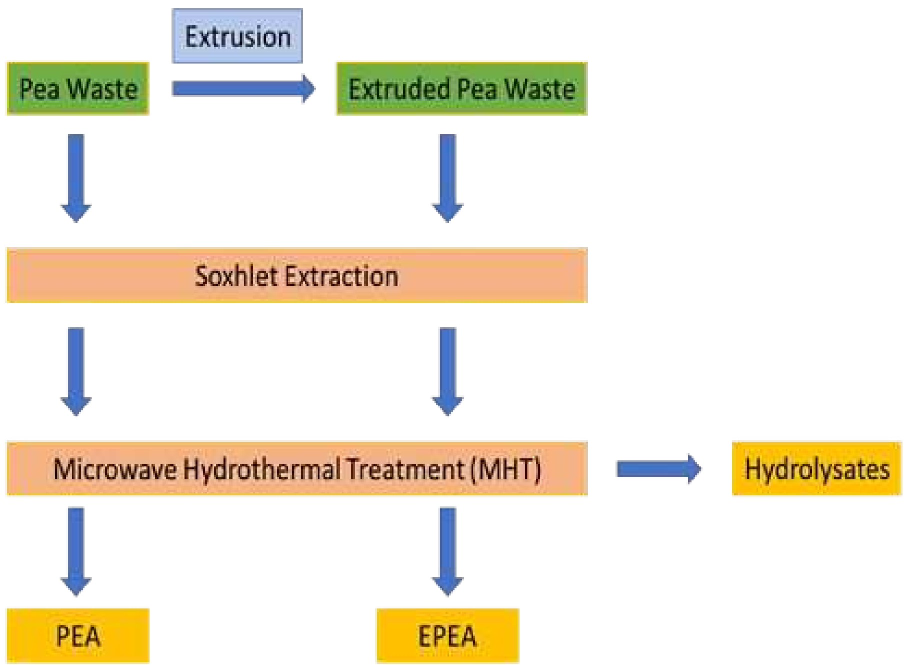

Figure 1. Process diagram to produce fibrillated cellulose pea waste using MHT.

EXPERIMENTAL

Materials

Pea (*Pisum sativum)* waste including leaves, vines, stems (haulm) was collected immediately after harvest from farmland nearby York (England, United Kingdom). The fresh biomass was then passed through a twin-screw press juicer (Angelia, 7500 Series, 180W) with a continuous shearing force between the screws and barrel to obtain the extruded pea pulp. Subsequently, both non-extruded pea waste and pressed pea waste were dried at room temperature for 2 weeks, milled in a knife miller (Retsch™ Knife Mill Grindomix GM300) and sieved (200 µm). The samples were subjected to Soxhlet extraction (ethanol, 24 h) to remove pigments and other organic compounds prior to the final microwave hydrothermal treatment (see Figure 1). The pea celluloses treated without extrusion pretreatment were coded PEA whereas, the extruded pretreated pea celluloses were coded EPEA. All solvents used were analytical or high-performance liquid chromatography (HPLC) grade and purchased from Sigma-Aldrich or Fisher Scientific.

The appropriate raw materials (either PEA or EPEA) were processed with a CEM Mars 6® closed vessel Microwave, operating in 1200 W, 2.45 GHz. EasyPrep Plus® closed vessels (Teflon, 100 mL). Dried pea or extruded pea (2 g) waste was mixed with distilled water (70 mL) with a ratio of 1: 35 (w/v) and subjected to MHT at different temperatures and, subsequently, freeze-dried for 24 h to obtain the desired MFC. Visual images of the product and hydrolysate are shown in Figure 2. The yield of the microfibrillated cellulose (MFC) was calculated according to equation (1):

$$\text{Yield\%} = (\text{mass of MFC} / \text{mass of dried raw material}) \times 100 \qquad \text{(eq. 1)}$$

The code used for each MFC is based on the MHT temperature used. For example, P120 refers to the non-extruded pea waste that was subjected to 120 °C MHT and EP160 refers to the extruded pea waste subjected to MHT at 160 °C.

Characterisation methods

For physicochemical characterization of PEA and EPEA, TGA, ATR-IR, powder XRD, Solid State 13C CPMAS NMR, SEM, TEM, HPLC and nitrogen adsorption porosimetry were performed. Crystallinity index was calculated using the NMR C4 peak separation method.[46] For TEM images, 2% mass ratio of the samples were dispersed in water with a 1500 W ultrasound bath for 20 min in order to get good clarity images. The widths of MFC were calculated by ImageJ software. Full instrument details are given in ESI. The water holding capacity (WHC: g_{H2O}/g_{sample}) was determined using literature methodology[47].

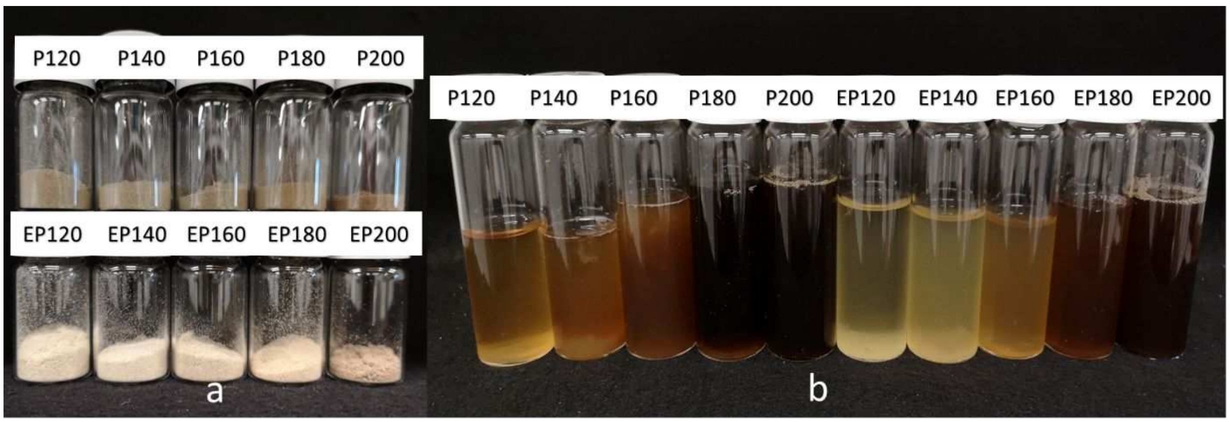

Figure 2. a. PEA and EPEA residues post MHT (120 –200 °C), b. hydrolysates from PEA and EPEA post MHT (120 –200 °C)

RESULTS AND DISCUSSION

Yield and CrI (Crystallinity Index)

The yields of PEA and EPEA produced at several MHT temperatures (120 ^{o}C-200 ^{o}C) are shown in Figure 3. During MHT, the yield of PEA and EPEA falls from 52.7 % to 32.4 % and from 66.0 % to 42.0 %, respectively as the processing temperature increases. In general, the EPEA samples display a higher yield than PEA at the same processing temperatures. The yield of PEA samples starts to decrease sharply (approximately 6.1 %) after 140 ^{o}C. For EPEA celluloses, the yield appears to remain relatively stable from 120 to 160 ^{o}C and decrease sharply. Higher yields with EPEA are probably due to the effect of extrusion which breaks the ordered structure of biomass and removes some hemicellulose and amorphous cellulosic matter by the shearing force between screws, biomass and barrel. Thus, the material is more cellulosic in character with less hydrolysable content.

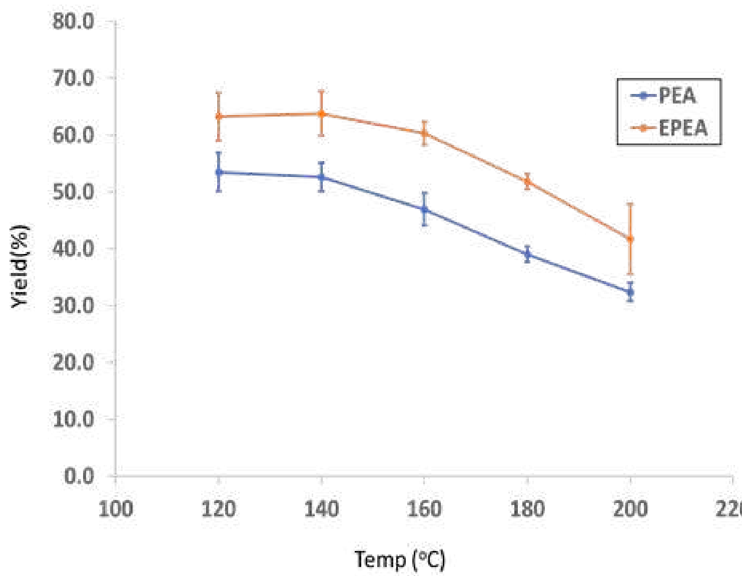

Figure 3. The final yield (%) of PEA and EPEA, Error bars represent standard deviation (n = 3).

The change in CrI (crystallinity index) of PEA and EPEA, determined from 13C CPMAS spectroscopy, with respect to MHT processing temperature are presented in Figure 4. The EPEA samples display a higher CrI than their corresponding PEA counterparts. With increasing MHT temperature, an obvious increase in the CrI is noted after 180 ^{o}C for PEA while the CrI of EPEA significantly increases after 160 ^{o}C (approx. Δ =1.65 %-6.3 % for PEA and 2.6 %–5 % for EPEA). These differences could be related to the two stages of the Hy-MASS concept[44], i.e., in the first step, the amorphous part in biomass (starch, hemicellulose) are selectively and progressively removed (scissoring) from the lignocellulosic matrix (120-180 ^{o}C)[48] which correlates well with compositional data: NMR,XRD,TGA (see later), and, in the second step, softened amorphous cellulose and lignin embedded in cellulose microfibrils is released through a proton transfer mechanism at higher temperatures (>180 ^{o}C). Extrusion as a pretreatment "softens" the material such that it can be hydrolyzed easier at a lower temperature (160 ^{o}C compared with 180 ^{o}C).

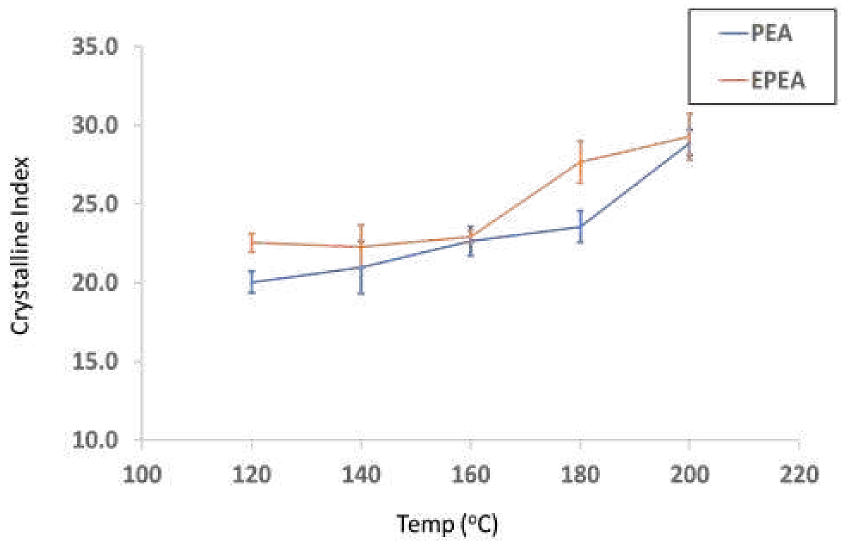

Figure 4. Crystallinity Index (CrI) calculated from solid state 13C CPMAS NMR data for PEA and EPEA, the error bars display standard deviation (n = 3).

Thermogravimetric analysis (TGA)

The TGA, and respective first derivatives (DTG), thermograms of PEA and EPEA cellulose are shown in Figure 5. PEA gave a higher residue content than EPEA (approximately 25.6% for PEA and 19.2% for EPEA), probably due to the fact that during extrusion water-soluble inorganic salts, for example, potassium, phosphorus, aluminium and iron, present in the biomass were removed, which correlated well with the ICP analysis (see Fig. S1). Furthermore, during MHT dissolvable inorganic minerals, except calcium, were removed and thus, no significant difference in the final residue mass was noted. Three main bands were observed from the DTG: i. loss of moisture and volatiles, (around 4% to 10%, Td=50-125 °C); ii. hemicellulose decomposition at front shoulder of the main peaks ranging from 250-280°C, and; iii. a mass loss (approximately 60%) between 280-390 °C due to cellulose decomposition. The peaks indicative of hemicellulose (250-280 °C) for both PEA and EPEA samples started to disappear with increasing MHT temperature and at 200 °C these peaks were no longer detectable (see blue arrows of DTG of PEA and EPEA in Figure 5). The decomposition temperatures of cellulose are shifted to higher temperatures (see black arrows of DTG of PEA and EPEA in Figure.5) with increasing MHT temperature, i.e., for non-extruded pea waste: native PEA (Td,313.2 °C); P120 (Td,344.1 °C); P140 (Td,346.8 °C); P160 (Td,351.3 °C); P180 (Td,365.8 °C); P200 (Td,373.9 °C), and for; extruded pea waste: native EPEA (Td,335.3 °C); EP120 (Td,345 °C); EP140 (Td,345.7 °C); EP160 (Td,354 °C); EP180 (Td,364 °C); EP200 (Td,373.2 °C), suggesting depletion of amorphous regions of cellulose fibrils [49] whilst retention of highly compact crystalline cellulose resulting in higher decomposition temperature. EPEA samples gave a higher decomposition temperature than their PEA counterparts showing the effectiveness of pretreatment.

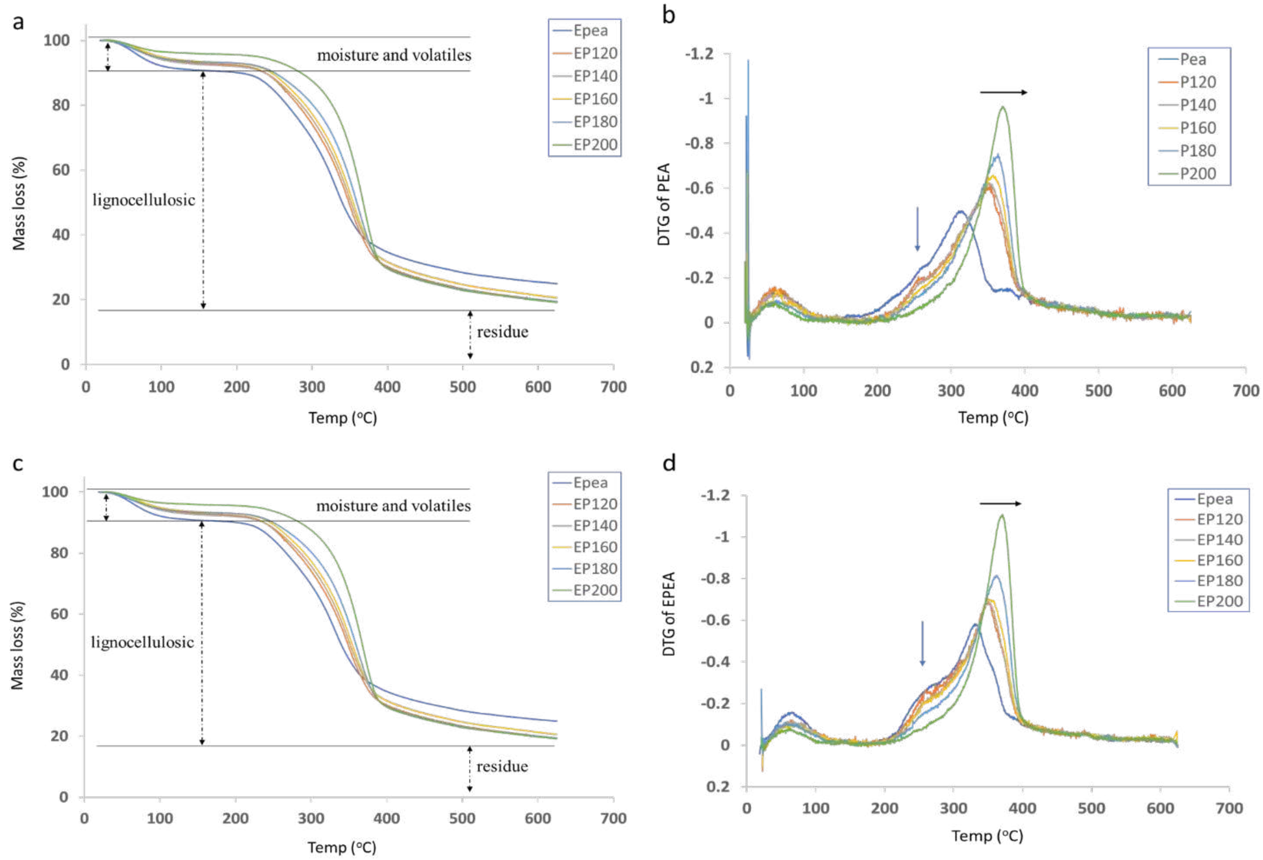

Figure 5. TGA thermograms of PEA and EPEA: a) TG of PEA, b) DTG of PEA, c) TG of EPEA and d) DTG of EPEA.

X-Ray powder diffraction analysis (XRD)

The XRD patterns of PEA and EPEA are shown in Figure 6. Characteristic peaks for crystalline cellulose peaks were observed (2θ: 16.5°, 22.5° and 34.5°) and with higher MHT temperature the crystalline diffraction peaks at 16.5° seemed to be more intense which revealed higher crystallinity (as already evidenced by 13C CPMAS in Figure. 4). These results indicate that after high temperature MHT both PEA and EPEA samples have higher decomposition temperatures indicative of an increase in the degree of crystallinity, loss of amorphous cellulose and removal of hemicellulosic impurities. The additional peaks at 15.1°, 24.4° and 30° are suspected to be insoluble calcium salts (e.g. CaC_2O_4) which exist in plant cell wall and vacuoles.[50] With the increasing MHT the XRD patterns for calcium oxalate in both PEA and EPEA samples became more intense due to the hydrolysis of amorphous polysaccharides and organic molecules from the lignocellulosic matrix. Also, the EPEA samples show a higher crystallinity and more intense calcium salts peaks than the non-extruded PEA, probably due to the extrusion disrupting cell wall structure of pea waste and aiding leaching of amorphous contents and soluble salts.

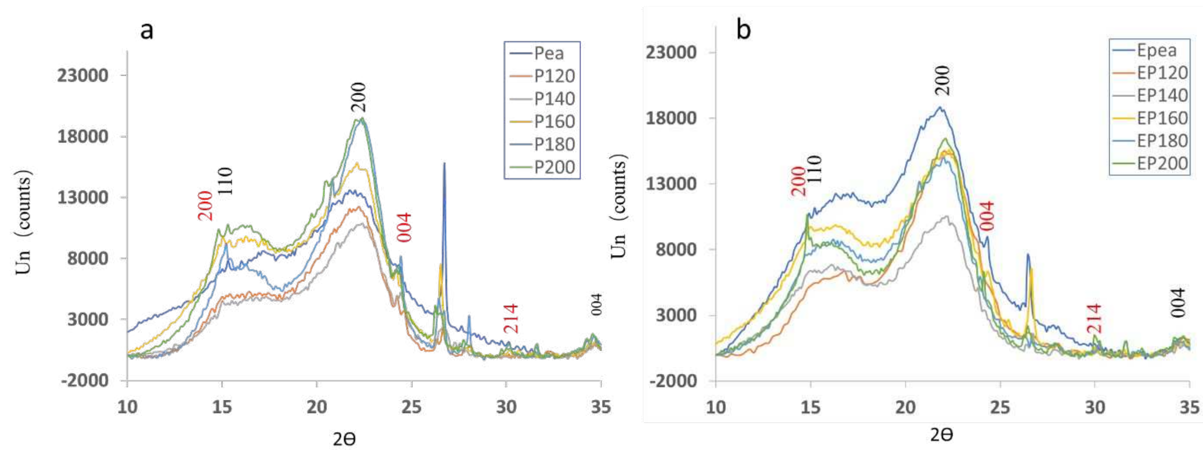

Figure 6. XRD diffractograms of a) PEA and b) EPEA varying from 120 to 200 ^oC. The cellulose peaks are shown in black and CaC_2O_4 peaks in red Planes.

ATR-IR

The ATR-IR analysis provides evidence for the presence of cellulose as the main component of the resulting product, as well as hemicellulose/lignin (see Figure 7). The O-H stretching vibration at about 3300 cm^{-1} was correlated to the hydroxyl moieties in cellulose I.[51] Bands at 2920 cm^{-1} refer to C-H stretch from cellulose/hemicellulose. The absorption bands at 1735 cm^{-1} were attributed to the carbonyl group from residual hemicellulose and lignin present in PEA and EPEA. The intensity of these bands decrease with increasing MHT temperature indicating that hemicellulose/lignin were gradually removed from cellulose during the microwave treatment.[52] Minor O-H bending vibration at about 1620 cm^{-1} was attributed to bonded water existing in the material. The bands at 1030 cm^{-1} corresponded to C–O and C-C stretching[53] confirming the presence of cellulose in PEA and EPEA, which became more evident at higher MHT temperatures since the non-cellulosic matter was gradually removed and therefore showed a purer cellulose spectrum.

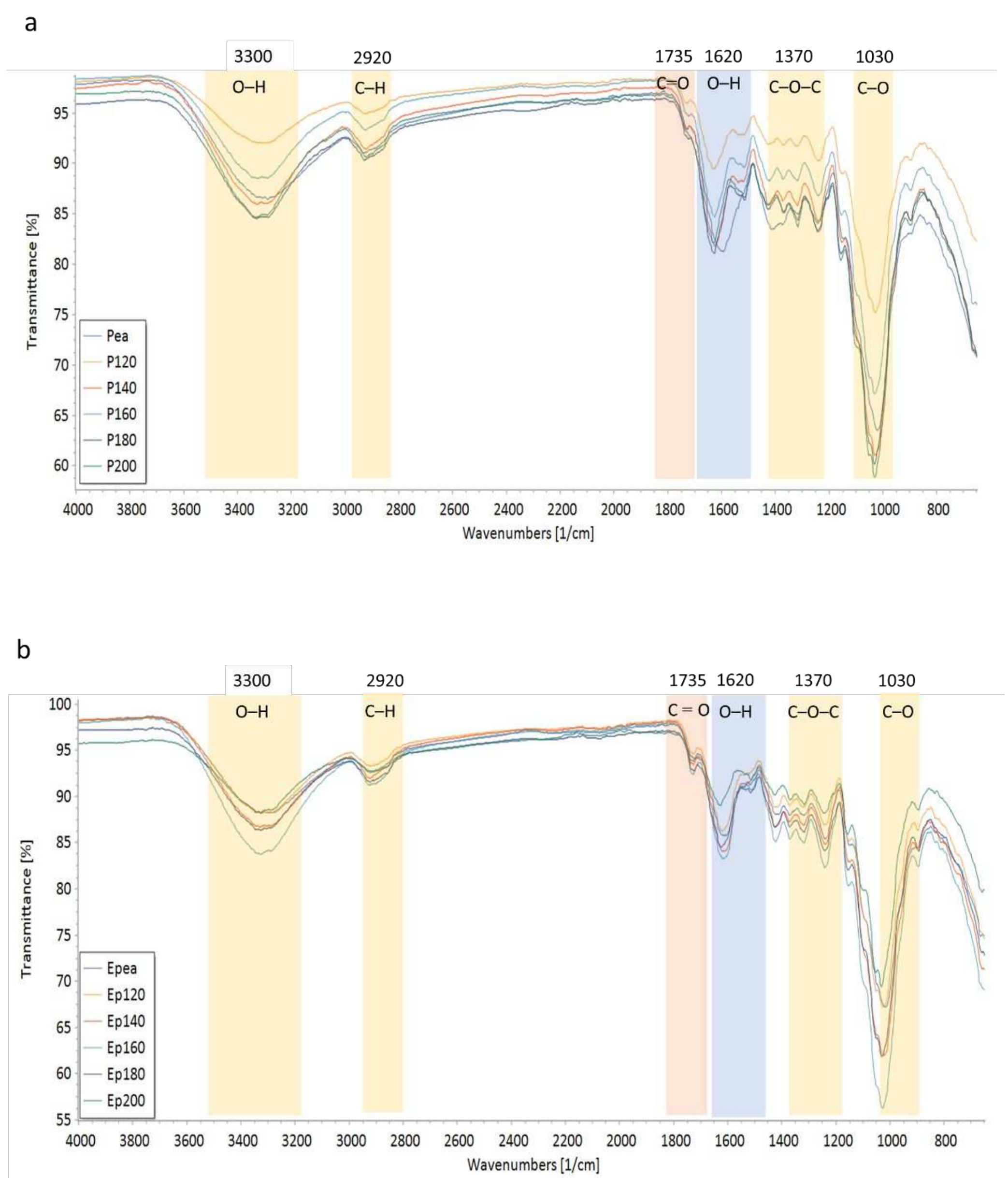

Figure 7. ATR-IR of a) PEA and b) EPEA varying from 120 to 200 °C.

Solid state 13C CPMAS NMR

The stacked 13C CPMAS spectra of PEA and EPEA samples with respect to increasing MHT temperature are shown in Figure 8. The signal at 175 ppm corresponds to the carbonyl carbon of carbonyl/carboxylic groups present in strongly bound cell wall polysaccharides (e.g. hemicelluloses) in pea waste.[54] The signals for cellulose carbons (C1 to C6)[55-58] are shown ranging from 110 ppm to 60 ppm. The peaks at 20 ppm may be attributed to acetyl group in polysaccharides (e.g. hemicelluloses) existing in the pea waste.[59-64] With increasing MHT temperature the signals of hemicellulose and/or lignin started to disappear especially after 180 °C, indicative of hydrolysis and depolymerization of the non-cellulosic matter[65]. At the same time, a significant change in cellulose structure was observed; the ratio of cellulosic surface/amorphous in C4 and C6 (84 ppm and 62 ppm, respectively) and interior/crystalline in C4 and C6 (89 ppm and 65 ppm, respectively)[66] was observed (arrows in yellow area Figure 8). The peaks representing crystalline regions starts to increase whilst the amorphous peaks start to reduce. This suggests that amorphous parts from the cellulose surface were also gradually hydrolyzed by MHT and the crystalline character of cellulose increased. These results correlate well with thermogravimetric data reported earlier and HPLC results to be discussed later.

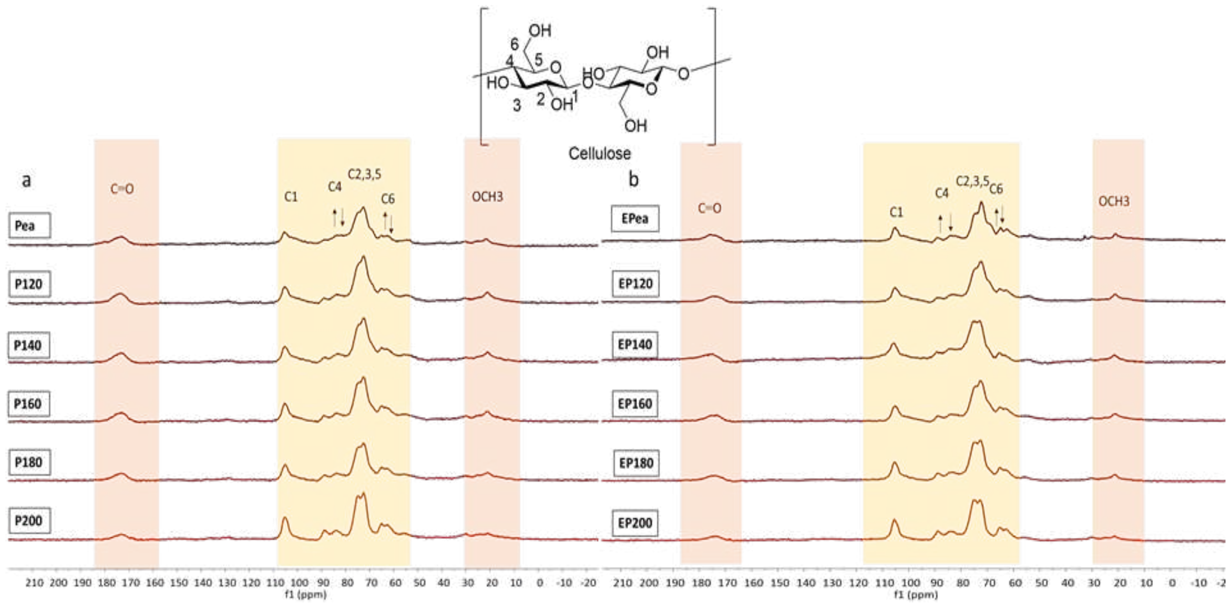

Figure 8. 13C CPMAS NMR spectra of a) PEA and b) EPEA samples with a labelled illustration of a cellulose moiety. Arrows show the ratio of crystalline/interior: amorphous/surface cellulose

TEM and SEM

Microfibrillated cellulose (MFC) and cellulose nanocrystals (CNC) were successfully evidenced by TEM through measurement of their fibril dimensions (Figure 9). In MFC the microfibrils and elementary fibrils (3–5 nm in width and a few µm in length) in both amorphous and crystalline regions[66-68] were present. The cellulose nanocrystals (width 5–70 nm and length <500 nm) which originated from crystalline regions of elementary fibrils were found in EP180, P200 and EP200 after the hydrolysis of amorphous regions at high temperature (above 180 °C) (see ESI Figure S2). This further confirmed the effect of the Hy-MASS concept, i.e. during MHT non-cellulosic biopolymers and amorphous regions of cellulose are hydrolyzed and cellulose nanocrystals are released above 180 ^{o}C.[69] Comparison of the two samples revealed that the EPEA series displayed a narrower width than their non-extruded counterparts (difference of *ca.* 2-4 nm). Also, nanocrystals were detected only in EPEA samples at 180 ^{o}C possibly implying that amorphous regions of pea cellulose were breached during extrusion and thus became easier to hydrolyse during MHT.

The grey regions which surround the nanofibrils are possibly residual amorphous matter (mainly include hemicellulose, lignin and some probably amorphous superficial cellulose),[44] with increasing MHT temperature, the gradual removal of grey regions occurred but some still persisted entangled with the nanofibrils and crystals even at a temperature of 200 ^{o}C (see ESI Figure S2). It could be that hemicellulose were "scissored" gradually during MHT but the residual lignin fragments could not be totally removed or the pseudo-lignin which is defined "an aromatic material that yields a positive Klason lignin value that is not derived from native lignin" were formed during the (MHT) process.[70] Interestingly, the extruded samples presented a less dark grey area than compared with their non-extruded counterparts. These result also prove that there are two steps in MHT: i. the outside amorphous regions in microfibrillated cellulose were "cut" progressively by microwave treatment up to 180 ^{o}C, and; ii. the nanocrystals which existed in elementary fibrils were released after 180–200 °C.

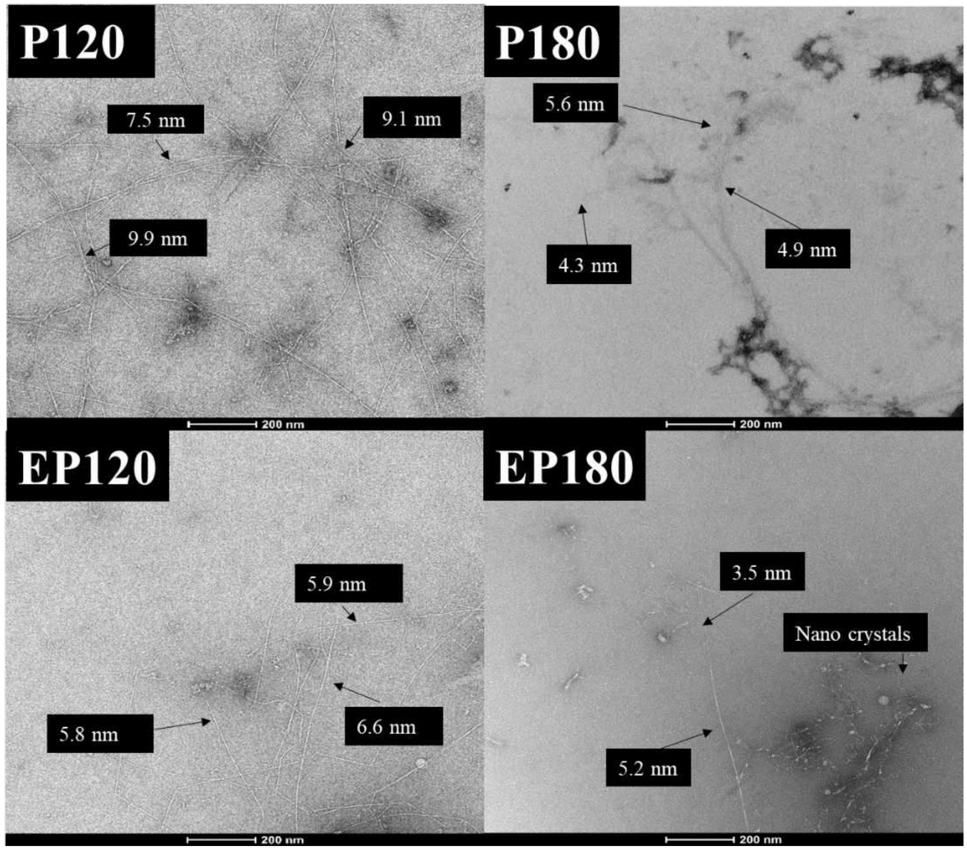

Figure 9. TEM images of PEA (120 °C,180 °C) and EPEA ((120 °C,180 °C)) samples (scale bar = 200 nm). The width of the MFC were labeled.

The SEM images from the surfaces of PEA and EPEA varying from 120 to 200 °C are shown in Figure 10. In the PEA samples, the fibre matrix presented a rough and more intact structure whilst the EPEA samples displaed smoother, thinner and heavily distorted fibres due to high shear created by extrusion. The EPEA samples tended to exhibit a more porous and corrugated surface, implying that the pretreatment made it easier for MHT to disrupt the tissue network of MFC.[71]

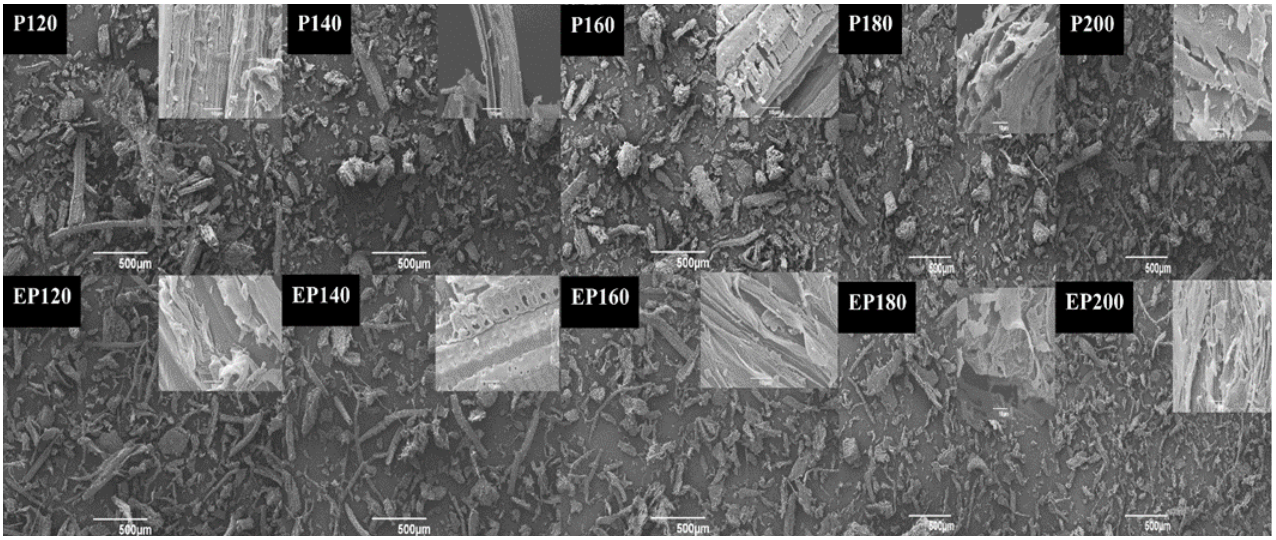

Figure 10. Morphological features of PEA and EPEA varying from 120 °C to 200 °C (scale bar = 500 μm). The additional SEM images are shown as insets (scale bar = 2 μm).

HPLC

The HPLC analyses of the hydrolysate obtained from MHT of the two samples (PEA and EPEA) are presented in Figure 11. In general, the sugar yield from PEA hydrolysate remained higher than the EPEA series. The yield of glucose decreased with increasing MHT processing temperature, 5-hydroxymethylfurfural (HMF) and furfural appeared after 180 °C. This can be related to the hydrolysis of polysaccharides in water below 220 °C.[49] Glucose could be derived from amorphous cellulose and hemicellulose, and 5-hydroxymethylfurfural (HMF) is considered the major secondary byproduct from glucose degradation. Xylose is mainly derived from residual hemicellulose since, the hydrolysis product was mainly from the amorphous part of the biomass and the crystalline region would not take part in the MHT reaction, thus the high amount of amorphous cellulose and hemicellulose would induce a higher sugar yield. After 180 °C， the part of glucose converted to HMF led to a yield reduction. Conversely, the xylose conversion to furfural did not affect its yield, hence, it may be reasonable to suppose that with higher temperature, hemicellulose has a higher conversion to monosaccharides.[72]

a

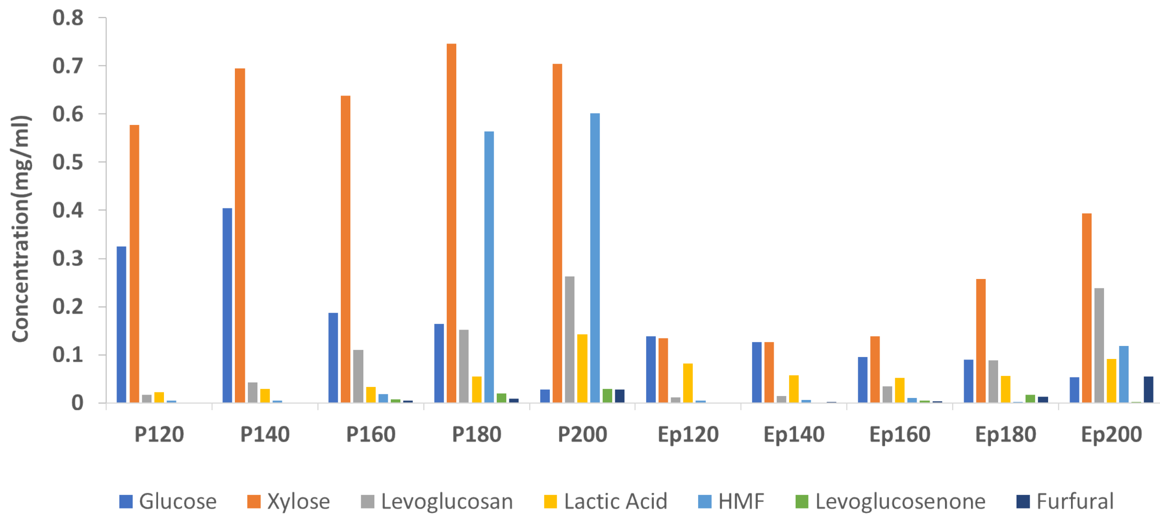

b

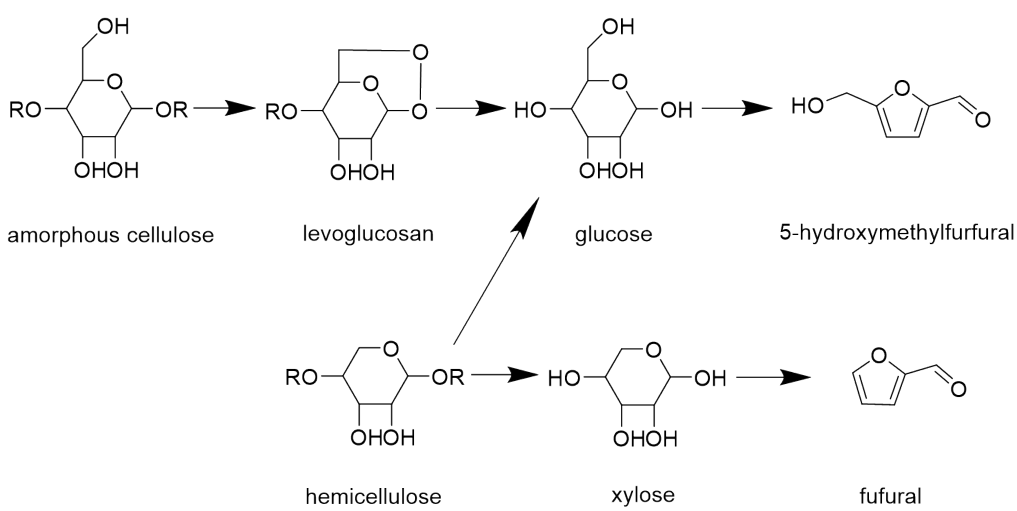

Figure 11. HPLC data for hydrolysates from PEA and EPEA after MHT (a) Products and subproducts from lignocellulosic, (b) conversion pathways to 5-HMF and furfural.

Water Holding Capacity (WHC)

The water holding capacity (WHC) of cellulose samples is shown in Figure 12. Both types of starting material (native biomass) have lower hydration capacity compared to their MFC products. The EPEA samples displayed a higher WHC than their non-extruded PEA counterparts (approximately 5% to 15% higher). It is well known that insoluble cellulose can hold water by absorbing water in their fibril network through swelling properties,[44] and the water holding capacity of MFC is related to the particle size and specific surface area.[47] During the gradual selective removal of amorphous cellulose by microwave treatment, particle size diminished and consequently the surface area of cellulose increased, improving hydration capacity. However, the water holding capacity of PEA and EPEA samples remained constant irrespective of MHT temperature (7 g and 8 g, respectively) which may due to the higher crystalline index of cellulose making it more hydrophobic.

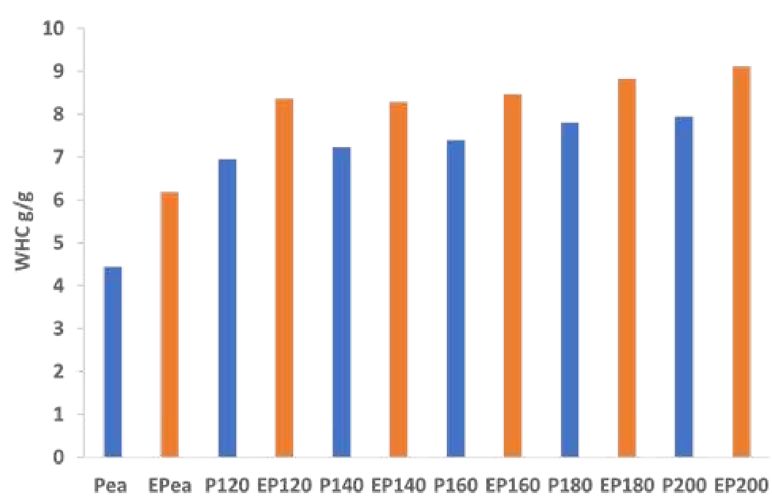

Figure 12. WHC of PEA and EPEA (g of water per g of dry sample). Values are average of duplicate experiments.

N_2 Adsorption porosimetry

The BET surface area, BJH average pore size and BJH pore volume for PEA and EPEA samples are shown in Figure 13. Both types of MFC display considerable surface area and porosity. For PEA samples, the BET specific surface area decreases initially up to 160 ^oC, and then increases from 160 to 200 ^oC; the BET surface area of EPEA samples decreased significantly from 120 to 160 ^oC (30 to 15 m^2/g) and then rose from 160 to 200 ^oC (15 to 37 m^2/g) which agrees with the scissoring of amorphous hemicellulose and lignin from cellulosic matrix. In general, EPEA samples displayed a higher BET surface area than their PEA counterparts (about 2-30 m^2/g higher), which could be explained by the destructive nature of the extrusion process destroying the original lignocellulosic construct. [66,73] The BJH average pore size was approximately 10 nm (between 2 and 50 nm) and thus these materials can be classified as mesoporous. [44] The pore volume of both samples presents a same pattern as for BET surface area: the pore volume of PEA and EPEA samples slightly decrease at first but then increase. The decrease in pore volume at may be associated with pores collapsing or becoming blocked which then become unblocked (melting and leaching of material from within pores) at higher MHT temperatures. Nevertheless, even though some useful information was obtained from N_2 adsorption porosimetry, this method is not the optimum technique for the analysis of "soft materials" such as cellulose since hornification, bound water and other artefacts can affect the results.

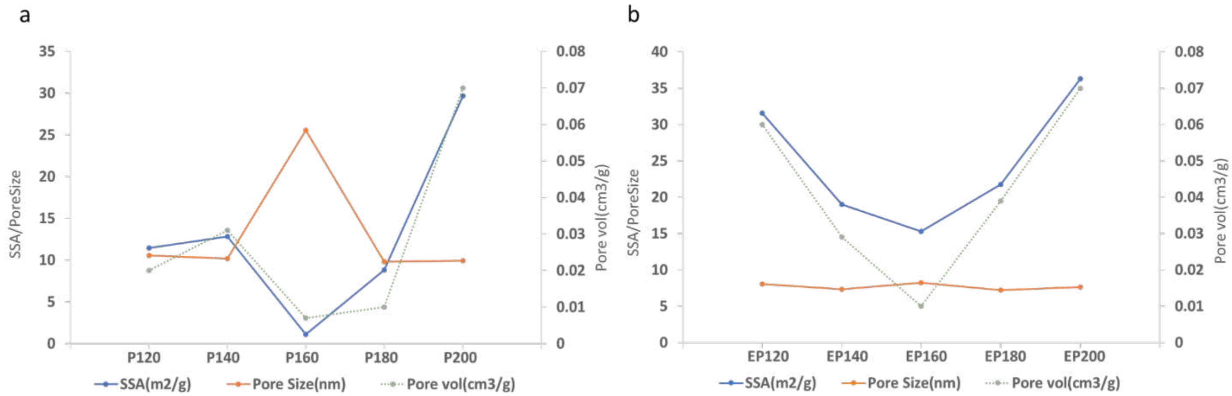

Figure 13. Porosimetry data (BET Specific surface area – SSA, BJH pore volume and BJH average pore size) for PEA (a) and EPEA (b) samples.

CONCLUSIONS

The feasibility of adopting twin-screw extrusion as a pretreatment method followed by microwave hydrothermal treatment (MHT) to produce mesoporous MFC from waste pea biomass is demonstrated. The amorphous regions in both samples were hydrolyzed in two stages during the microwave treatment evidencing the HyMass concept and scissoring of cellulose. The EPEA samples presented relatively better physical properties (high crystalline index, high hydration capacity and large surface area) than their non-extruded PEA counterparts. Thus, within the concept of green and sustainable chemistry, utilisation of waste as a feedstock (namely, unavoidable food supply chain wastes) within the concept of a biorefinery could be used to yield chemicals, materials (in this case MFC) and bioenergy. MFC production is much simpler and more environmentally-friendly than compared with conventional processing of wood pulp.

ASSOCIATED CONTENT

Supporting Information

The Supporting Information is available free of charge on the ACS Publications website at

Experimental details, Figures S1, S2

AUTHOR INFORMATION

Corresponding Author

* E-mail: avtar.matharu@york.ac.uk (Avtar S. Matharu)

Notes

The authors declare no competing financial interest.

ORCID

Avtar S. Matharu: https://orcid.org/0000-0002-9488-565X

ACKNOWLEDGEMENT

ASM and TIJD would like to thank EPSRC (Whole systems understanding of unavoidable food supply chain wastes for re-nutrition EP/P008771/1) for funding. YG would like to thank Dr Meg Stark and Dr Karen Hodgkinson for TEM and SEM analysis and Dr Hannah Briers for HPLC sugar analysis.

REFERENCES

(1) Verma, N.; Bansal, M. C.; Kumar, V. Pea peel Waste: A lignocellulosic waste and its utility in cellulase production by Trichoderma reesei under solid state cultivation. *BioResources,* **2011,** 6 (2), 1505-1519.

(2) Choi, W. S.; Han, J. H. Physical and mechanical properties of pea-protein-based edible films. *Food science,* **2001,** 66 (2), 319-322.

(3) Agriculture in the United Kingdom. https://www.gov.uk/government/collections/agriculture-in-the-united-kingdom (accessed January 2019).

(4) Nimbalkar, P. R.; Khedkar, M. A.; Chavan, P. V.; Bankar, S. B. Biobutanol production using pea pod waste as substrate: Impact of drying on saccharification and fermentation. *Renew. Energ.,* **2018,** 117, 520-529.

(5) Xia, H.; Houghton, J. A.; Clark, J. H.; Matharu, A. S. Potential Utilization of Unavoidable Food Supply Chain Wastes–Valorization of Pea Vine Wastes. *ACS Sustainable Chem. & Eng.,* **2016,** 4 (11), 6002-6009.

(6) Sharma, R.; Rawat, R.; Bhogal, R. S.; Oberoi, H. S. Multi-component thermostable cellulolytic enzyme production by Aspergillus niger HN-1 using pea pod waste: Appraisal of hydrolytic potential with lignocellulosic biomass. *Process Biochem.,* **2015,** 50 (5), 696-704.

(7) Müsellim, E.; Tahir, M. H.; Ahmad, M. S.; Ceylan, S. Thermokinetic and TG/DSC-FTIR study of pea waste biomass pyrolysis. *Appl. Therm. Eng.,* **2018,** 137, 54-61.

(8) Gómez, L. D.; Vanholme, R.; Bird, S.; Goeminne, G.; Trindade, L. M.; Polikarpov, I.; Simister, R.; Morreel, K.; Boerjan, W.; McQueen-Mason, S. J. Side by Side Comparison of Chemical Compounds Generated by Aqueous Pretreatments of Maize Stover, Miscanthus and Sugarcane Bagasse. *BioEnergy Research,* **2014,** 7 (4), 1466-1480.

(9) Kim, J.-H.; Shim, B. S.; Kim, H. S.; Lee, Y.-J.; Min, S.-K.; Jang, D.; Abas, Z.; Kim, J. Review of nanocellulose for sustainable future materials. *International Journal of Precision Engineering and Manufacturing-Green Technology,* **2015,** 2 (2), 197-213.

(10) Hoeng, F.; Denneulin, A.; Bras, J. Use of nanocellulose in printed electronics: a review. *Nanoscale,* **2016,** 8 (27), 13131-13154.

(11) Kaushik, M.; Moores, A. nanocelluloses as versatile supports for metal nanoparticles and their applications in catalysis. *Green Chem.,* **2016,** 18 (3), 622-637.

(12) De France, K. J.; Hoare, T.; Cranston, E. D. Review of Hydrogels and Aerogels Containing Nanocellulose. *Chem. Mater.,* **2017,** 29 (11), 4609-4631.

(13) Du, H.; Liu, W.; Zhang, M.; Si, C.; Zhang, X.; Li, B. Cellulose nanocrystals and cellulose nanofibrils based hydrogels for biomedical applications. *Carbohyd. Polym.,* **2019,** 209, 130-144.

(14) Abdul Khalil, H. P. S.; Davoudpour, Y.; Saurabh, C. K.; Hossain, M. S.; Adnan, A. S.; Dungani, R.; Paridah, M. T.; Islam Sarker, M. Z.; Fazita, M. R. N.; Syakir, M. I.; Haafiz, M. K. M. A review on nanocellulosic fibres as new material for sustainable packaging: Process and applications. *Renew. Sust. Energ. Rev.,* **2016,** 64, 823-836.

(15) Moon, R. J.; Martini, A.; Nairn, J.; Simonsen, J.; Youngblood, J. Cellulose nanomaterials review: structure, properties and nanocomposites. *Chem. Soc. Rev.,* **2011,** 40 (7), 3941-3994.

(16) García, A.; Gandini, A.; Labidi, J.; Belgacem, N.; Bras, J. Industrial and crop wastes: A new source for nanocellulose biorefinery. *Ind. Crop Prod.,* **2016,** *93*, 26-38.

(17) Market resource report. https://www.marketsandmarkets.com/Market-Reports/nano-cellulose-market-56392090.html?gclid=EAIaIQobChMIq4Xdma-Q4AIVDrHtCh2aGgJQEAAYASAAEgKjtfD_BwE# (accessed 28/1/2019).

(18) Klemm, D.; Kramer, F.; Moritz, S.; Lindstrom, T.; Ankerfors, M.; Gray, D.; Dorris, A. Nanocelluloses: a new family of nature-based materials. *Angew. Chem. Int. Ed,* **2011,** 50 (24),5438-5466.

(19) Kargarzadeh, H.; Ahmad, I.; Thomas, S.; Dufresne, A., *Handbook of Nanocellulose and Cellulose Nanocomposites*. John Wiley & Sons: 2017,p 9-10.

(20) Matharu, A. S.; de Melo, E. M.; Remon, J.; Wang, S.; Abdulina, A.; Kontturi, E. Processing of citrus nanostructured cellulose: a rigorous design-of-experiment study of the hydrothermal microwave-assisted selective scissoring process. *ChemSusChem,* **2018,** 11 (8), 1344-1353.

(21) Reid, M. S.; Villalobos, M.; Cranston, E. D. Benchmarking Cellulose Nanocrystals: From the Laboratory to Industrial Production. *Langmuir,* **2017,** 33 (7), 1583-1598.

(22) Rebouillat, S.; Pla, F. State of the Art Manufacturing and Engineering of Nanocellulose: A Review of Available Data and Industrial Applications. *Journal of Biomaterials and Nanobiotechnology,* **2013,** 04 (02), 165-188.

(23) Wilkinson, S.; Greetham, D.; Tucker, G. A. Evaluation of different lignocellulosic biomass pretreatments by phenotypic microarray-based metabolic analysis of fermenting yeast. *Biofuel Research Journal,* **2016,** 3 (1), 357-365.

(24) Kudakasseril Kurian, J.; Raveendran Nair, G.; Hussain, A.; Vijaya Raghavan, G. S. Feedstocks, logistics and pre-treatment processes for sustainable lignocellulosic biorefineries: A comprehensive review. *Renew. Sust. Energ. Rev.,* **2013,** 25, 205-219.

(25) Chen, H.; Liu, J.; Chang, X.; Chen, D.; Xue, Y.; Liu, P.; Lin, H.; Han, S. A review on the pretreatment of lignocellulose for high-value chemicals. *Fuel Process. Technol.,* **2017,** 160, 196-206.

(26) Rajinipriya, M.; Nagalakshmaiah, M.; Robert, M.; Elkoun, S. Importance of Agricultural and Industrial Waste in the field of nanocellulose and recent industrial developments of wood based nanocellulose: a review. *ACS Sustainable Chem. & Eng.,* **2018,** 6 (3), 2807-2828.

(27) An, Y.-X.; Zong, M.-H.; Wu, H.; Li, N. Pretreatment of lignocellulosic biomass with renewable cholinium ionic liquids: Biomass fractionation, enzymatic digestion and ionic liquid reuse. *Bioresour. Technol.,* **2015,** 192, 165-171.

(28) Chandra, R. P.; Arantes, V.; Saddler, J. Steam pretreatment of agricultural residues facilitates hemicellulose recovery while enhancing enzyme accessibility to cellulose. *Bioresour. Technol.,* **2015,** 185,302-307.

(29) Michalska, K.; Miazek, K.; Krzystek, L.; Ledakowicz, S. Influence of pretreatment with Fenton's reagent on biogas production and methane yield from lignocellulosic biomass. *Bioresour. Technol.,* **2012,** 119,72-78.

(30) George, A.; Brandt, A.; Tran, K.; Zahari, S. M. S. N. S.; Klein-Marcuschamer, D.; Sun, N.; Sathitsuksanoh, N.; Shi, J.; Stavila, V.; Parthasarathi, R.; Singh, S.; Holmes, B. M.; Welton, T.; Simmons, B. A.; Hallett, J. P. Design of low-cost ionic liquids for lignocellulosic biomass pretreatment. *Green Chem.,* **2015,** 17 (3), 1728-1734.

(31) Xu, F.; Sun, J.; Konda, N. V. S. N. M.; Shi, J.; Dutta, T.; Scown, C. D.; Simmons, B. A.; Singh, S. Transforming biomass conversion with ionic liquids: process intensification and the development of a high-gravity, one-pot process for the production of cellulosic ethanol. *Energ. Environ. Sci.,* **2016,** 9 (3), 1042-1049.

(32) Yan, Z.; Li, J.; Chang, S.; Cui, T.; Jiang, Y.; Yu, M.; Zhang, L.; Zhao, G.; Qi, P.; Li, S. Lignin relocation contributed to the alkaline pretreatment efficiency of sweet sorghum bagasse. *Fuel,* **2015,** 158, 152-158.

(33) Laurens, L. M. L.; Nagle, N.; Davis, R.; Sweeney, N.; Van Wychen, S.; Lowell, A.; Pienkos, P. T. Acid-catalyzed algal biomass pretreatment for integrated lipid and carbohydrate-based biofuels production. *Green Chem.,* **2015,** 17 (2), 1145-1158.

(34) Murciano Martínez, P.; Bakker, R.; Harmsen, P.; Gruppen, H.; Kabel, M. Importance of acid or alkali concentration on the removal of xylan and lignin for enzymatic cellulose hydrolysis. *Ind. Crop Prod.,* **2015,** 64,88-96.

(35) Zubrowska-Sudol, M.; Walczak, J. Effects of mechanical disintegration of activated sludge on the activity of nitrifying and denitrifying bacteria and phosphorus accumulating organisms. *Water Res.,* **2014,** 61,200-209.

(36) Hu, H.; Zhang, Y.; Liu, X.; Huang, Z.; Chen, Y.; Yang, M.; Qin, X.; Feng, Z. Structural changes and enhanced accessibility of natural cellulose pretreated by mechanical activation. *Polym. Bull.,* **2013,** 71 (2), 453-464.

(37) Anis, S.; Zainal, Z. A. Study on kinetic model of microwave thermocatalytic treatment of biomass tar model compound. *Bioresour. Technol.,* **2014,** 151, 183-90.

(38) Rouches, E.; Herpoël-Gimbert, I.; Steyer, J. P.; Carrere, H. Improvement of anaerobic degradation by white-rot fungi pretreatment of lignocellulosic biomass: A review. *Renew. Sust. Energ. Rev.,* **2016,** 59, 179-198.

(39) Alvira, P.; Negro, M. J.; Ballesteros, I.; González, A.; Ballesteros, M. Steam explosion for wheat straw pretreatment for sugars production. *Bioethanol,* **2016,** 2 (1), 66-75.

(40) Lopez-Linares, J. C.; Ballesteros, I.; Touran, J.; Cara, C.; Castro, E.; Ballesteros, M.; Romero, I. Optimization of uncatalyzed steam explosion pretreatment of rapeseed straw for biofuel production. *Bioresour. Technol.,* **2015,** 190, 97-105.

(41) Chen, L.; Zhu, J. Y.; Baez, C.; Kitin, P.; Elder, T. Highly thermal-stable and functional cellulose nanocrystals and nanofibrils produced using fully recyclable organic acids. *Green Chem.,* **2016,** 18 (13), 3835-3843.

(42) Iskak, N. A. M.; Julkapli, N. M.; Hamid, S. B. A. Understanding the effect of synthesis parameters on the catalytic ionic liquid hydrolysis process of cellulose nanocrystals. *Cellulose,* **2017,** 24 (6), 2469-2481.

(43) Satyamurthy, P.; Jain, P.; Balasubramanya, R. H.; Vigneshwaran, N. Preparation and characterization of cellulose nanowhiskers from cotton fibres by controlled microbial hydrolysis. *Carbohyd. Polym.,* **2011,** 83 (1), 122-129.

(44) de Melo, E. M.; Clark, J. H.; Matharu, A. S. The Hy-MASS concept: hydrothermal microwave assisted selective scissoring of cellulose for in situ production of (meso)porous nanocellulose fibrils and crystals. *Green Chem.,* **2017,** 19 (14), 3408-3417.

(45) Duque, A.; Manzanares, P.; Ballesteros, M. Extrusion as a pretreatment for lignocellulosic biomass: Fundamentals and applications. *Renew. Energ.,* **2017,** 114, 1427-1441.

(46) Park, S.; Baker, J. O.; Himmel, M. E.; Parilla, P. A.; Johnson, D. K. Cellulose crystallinity index: measurement techniques and their impact on interpreting cellulase performance. *Biotechnology for biofuels,* **2010,** 3 (1),1-10.

(47) Zain, N. F.; Yusop, S. M.; Ahmad, I. Preparation and characterization of cellulose and nanocellulose from pomelo (Citrus grandis) albedo. *J. Nutr. Food Sci.,* **2014,** 5 (1),1-5.

(48) Tsubaki, S.; Azuma, J.-i., Application of microwave technology for utilization of recalcitrant biomass. In *Advances in induction and microwave heating of mineral and organic materials*, InTech: 2011,p 699-700.

(49) Fan, J.; De bruyn, M.; Budarin, V. L.; Gronnow, M. J.; Shuttleworth, P. S.; Breeden, S.; Macquarrie, D. J.; Clark, J. H. Direct Microwave-Assisted Hydrothermal Depolymerization of Cellulose. *J. Am. Chem. Soc.,* **2013,** 135 (32), 11728-11731.

(50) Hajir, M.; Graf, R.; Tremel, W. Stable amorphous calcium oxalate: synthesis and potential intermediate in biomineralization. *Chem. Commun. (Camb),* **2014,** 50 (49),6534-6536.

(51) Kumar, A.; Negi, Y. S.; Choudhary, V.; Bhardwaj, N. K. Characterization of cellulose nanocrystals produced by acid-hydrolysis from sugarcane bagasse as agro-waste. *Journal of Materials Physics and Chemistry,* **2014,** 2 (1), 1-8.

(52) Azadfar, M.; Gao, A. H.; Bule, M. V.; Chen, S. Structural characterization of lignin: a potential source of antioxidants guaiacol and 4-vinylguaiacol. *Int. J. Biol. Macromol.,* **2015,** 75, 58-66.

(53) Szymanska-Chargot, M.; Zdunek, A. Use of FT-IR spectra and PCA to the bulk characterization of cell wall residues of fruits and vegetables along a fraction process. *Food biophysics,* **2013,** 8 (1), 29-42.

(54) Tai, H.-C.; Li, G.-C.; Huang, S.-J.; Jhu, C.-R.; Chung, J.-H.; Wang, B. Y.; Hsu, C.-S.; Brandmair, B.; Chung, D.-T.; Chen, H. M. Chemical distinctions between Stradivari's maple and modern tonewood. *Proceedings of the National Academy of Sciences,* **2017,** 114 (1), 27-32.

(55) Kono, H.; Yunoki, S.; Shikano, T.; Fujiwara, M.; Erata, T.; Takai, M. CP/MAS 13C NMR study of cellulose and cellulose derivatives. 1. Complete assignment of the CP/MAS 13C NMR spectrum of the native cellulose. *J. Am. Chem. Soc.,* **2002,** 124 (25), 7506-7511.

(56) Söyler, Z.; Meier, M. A. R. Sustainable functionalization of cellulose and starch with diallyl carbonate in ionic liquids. *Green Chem.,* **2017,** 19 (16), 3899-3907.

(57) Simmons, T. J.; Mortimer, J. C.; Bernardinelli, O. D.; Poppler, A. C.; Brown, S. P.; deAzevedo, E. R.; Dupree, R.; Dupree, P. Folding of xylan onto cellulose fibrils in plant cell walls revealed by solid-state NMR. *Nat. Commun.,* **2016,** 7,1-9.

(58) Wang, T.; Yang, H.; Kubicki, J. D.; Hong, M. Cellulose Structural Polymorphism in Plant Primary Cell Walls Investigated by High-Field 2D Solid-State NMR Spectroscopy and Density Functional Theory Calculations. *Biomacromolecules,* **2016,** 17 (6),2210-2222.

(59) Vismara, E.; Gastaldi, G.; Valerio, A.; Bertini, S.; Cosentino, C.; Eisle, G. Alpha cellulose from industrial and agricultural renewable sources like short flax fibres, ears of corn and wheat-straw and its transformation into cellulose acetates. *J. Mater. Chem.,* **2009,** 19 (45),8678-8686.

(60) Tai, H. C.; Li, G. C.; Huang, S. J.; Jhu, C. R.; Chung, J. H.; Wang, B. Y.; Hsu, C. S.; Brandmair, B.; Chung, D. T.; Chen, H. M.; Chan, J. C. Chemical distinctions between Stradivari's maple and modern tonewood. *Proc. Natl. Acad. Sci. U. S. A.,* **2017,** *114* (1), 27-32.

(61) Zhu, W.; Westman, G.; Theliander, H. The molecular properties and carbohydrate content of lignins precipitated from black liquor. *Holzforschung,* **2015,** 69 (2),143-152.

(62) Sannigrahi, P.; Kim, D. H.; Jung, S.; Ragauskas, A. Pseudo-lignin and pretreatment chemistry. *Energ. Environ. Sci.,* **2011,** 4 (4), 1306-1310.

(63) Cheng, H. N.; Neiss, T. G. Solution NMR Spectroscopy of Food Polysaccharides. *Polym. Rev. (Philadelphia, PA, U. S.),* **2012,** 52 (2), 81-114.

(64) Foston, M.; Katahira, R.; Gjersing, E.; Davis, M. F.; Ragauskas, A. J. Solid-state selective (13)C excitation and spin diffusion NMR to resolve spatial dimensions in plant cell walls. *J. Agric. Food Chem.,* **2012,** 60 (6),1419-1427.

(65) Balu, A. M.; Budarin, V.; Shuttleworth, P. S.; Pfaltzgraff, L. A.; Waldron, K.; Luque, R.; Clark, J. H. Valorisation of orange peel residues: waste to biochemicals and nanoporous materials. *ChemSusChem,* **2012,** 5 (9), 1694-1697.

(66) Cheng, G.; Zhang, X.; Simmons, B.; Singh, S. Theory, practice and prospects of X-ray and neutron scattering for lignocellulosic biomass characterization: towards understanding biomass pretreatment. *Energ. Environ. Sci.,* **2015,** 8 (2), 436-455.

(67) Sofla, M. R. K.; Brown, R. J.; Tsuzuki, T.; Rainey, T. J. A comparison of cellulose nanocrystals and cellulose nanofibres extracted from bagasse using acid and ball milling methods. *Advances in Natural Sciences: Nanoscience and Nanotechnology,* **2016,** 7 (3),1-9 .

(68) Zhu, H.; Fang, Z.; Preston, C.; Li, Y.; Hu, L. Transparent paper: fabrications, properties, and device applications. *Energ. Environ. Sci.,* **2014,** 7 (1), 269-287.

(69) Flórez, N.; Conde, E.; Domínguez, H. Microwave assisted water extraction of plant compounds. *J. Chem. Technol. Biotechnol.,* **2015,** 90 (4), 590-607.

(70) Hu, F.; Jung, S.; Ragauskas, A. Pseudo-lignin formation and its impact on enzymatic hydrolysis. *Bioresour. Technol,* **2012,** 117, 7-12.

(71) Su, T. C.; Fang, Z.; Zhang, F.; Luo, J.; Li, X. K. Hydrolysis of Selected Tropical Plant Wastes Catalyzed by a Magnetic Carbonaceous Acid with Microwave. *Sci Rep,* **2015,** 5,1-14.

(72) Mamman, A. S.; Lee, J. M.; Kim, Y. C.; Hwang, I. T.; Park, N. J.; Hwang, Y. K.; Chang, J. S.; Hwang, J. S. Furfural: Hemicellulose/xylosederived biochemical. *Biofuels, Bioproducts and Biorefining: Innovation for a sustainable economy,* **2008,** 2 (5), 438-454.

(73) Viamajala, S.; Donohoe, B. S.; Decker, S. R.; Vinzant, T. B.; Selig, M. J.; Himmel, M. E.; Tucker, M. P., Heat and mass transport in processing of lignocellulosic biomass for fuels and chemicals. In *Sustainable biotechnology*, Springer: 2010; p 1-18.

TOC Graphic

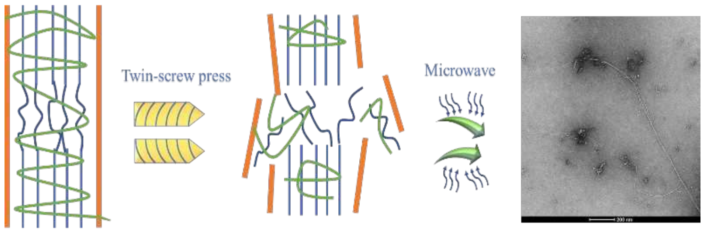

Defibrillation of twin-screw extruded spent pea biomass via Hydrothermal Microwave Treatment (MHT) to yield micro-fibrillated cellulose (MFC)

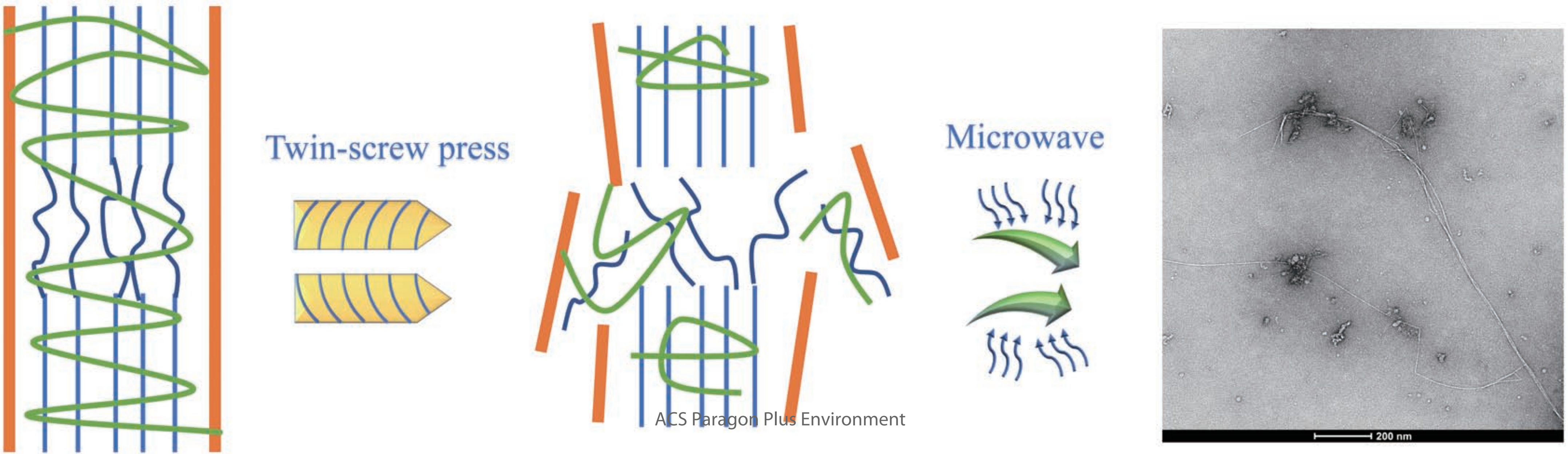
Twin-screw press
Microwave
200 nm